Architectural changes in superficial and deep compartments of the tibialis anterior during electrical stimulation over different sites

Architectural changes in superficial and deep compartments of the tibialis anterior during electrical stimulation over different sites

Marco Carbonaro, Olivier Seynnes, Nicola A. Maffiuletti, Chiara Busso, Marco A. Minetto, and Alberto Botter, *Member*, *IEEE*

***Abstract*— Electrical stimulation is widely used in rehabilitation to prevent muscle weakness and to assist the functional recovery of neural deficits. Its application is however limited by the rapid development of muscle fatigue due to the non-physiological motor unit (MU) recruitment. This issue can be mitigated by interleaving muscle belly (mStim) and nerve stimulation (nStim) to distribute the temporal recruitment among different MU groups. To be effective, this approach requires the two stimulation modalities to activate minimally-overlapped groups of MUs. In this manuscript, we investigated spatial differences between mStim and nStim MU recruitment through the study of architectural changes of superficial and deep compartments of tibialis anterior (TA). We used ultrasound imaging to measure variations in muscle thickness, pennation angle, and fiber length during mStim, nStim, and voluntary (Vol) contractions at 15% and 25% of the maximal force. For both contraction levels, architectural changes induced by nStim in the deep and superficial compartments were similar to those observed during Vol. Instead, during mStim superficial fascicles underwent a greater change compared to those observed during nStim and Vol, both in absolute magnitude and in their relative differences between compartments. These observations suggest that nStim results in a distributed MU recruitment over the entire muscle volume, similarly to Vol, whereas mStim preferentially activates the superficial muscle layer. The diversity between spatial recruitment of nStim and mStim suggests the involvement of different MU populations, which justifies strategies based on interleaved nerve/muscle stimulation to reduce muscle fatigue during electrically-induced contractions of TA.**

***Index Terms*— Electrical stimulation, spatial recruitment, muscle architecture, muscle fatigue, ultrasonography.**

This study was supported by University of Turin (Fondo per la Ricerca Locale - ex-60%) and by the Italian Ministry of Education, University and Research (MIUR) under the programme "Dipartimenti di Eccellenza ex L. 232/2016" to the Department of Surgical Sciences, University of Turin.

M. Carbonaro and A. Botter are with the Laboratory for Engineering of the Neuromuscular System (LISiN), Department of Electronics and Telecommunications, Politecnico di Torino, and with the PoliToBIOMed Lab, Politecnico di Torino, 10129 Turin, Italy (e-mail: marco.carbonaro@polito.it and alberto.botter@polito.it).

O. Seynnes is with the Norwegian School of Sport Sciences, Oslo, Norway (e-mail: olivier.seynnes@nih.no).

N.A. Maffiuletti is with the Human Performance Lab, Schulthess Clinic, Zurich, Switzerland (e-mail: nicola.maffiuletti@kws.ch).

C. Busso and M.A. Minetto are with the Division of Physical Medicine and Rehabilitation, Department of Surgical Sciences, University of Turin, Corso Dogliotti 14, 10126, Turin, Italy (e-mail: chiara.busso@unito.it and marco.minetto@unito.it).

I. Introduction

ELECTRICAL stimulation of skeletal muscles is widely used to prevent muscle weakness and atrophy, to improve muscle function (e.g. in rehabilitation and training [1]) or to compensate for functional deficits after neural damage (e.g. to improve gait quality in post-stroke patients [2]). Muscle contractions can be evoked by delivering electrical pulses over the trunk of peripheral nerves or to the terminal nerve branches at the muscle level. The former type of stimulation is typically referred to as nerve trunk stimulation (nStim), while the latter is called neuromuscular electrical stimulation or muscle belly stimulation (mStim).

A well-known factor limiting the clinical use of electrical stimulation is the development of muscle fatigue , i.e. a decline in the capacity of muscle to generate force, that is particularly marked and fast in stimulated contractions [3]. This performance reduction, also referred to as “fatigability” [4], is largely due to the non-physiological pattern of motor unit (MU) recruitment occurring in electrically-induced contractions. Unlike voluntary contractions, the order of recruitment of MUs does not follow the Henneman’s size principle [5] and depends on the electrode location and configuration [6]–[10]. Additionally, MUs tend to be recruited synchronously with the stimulation frequency [11], requiring higher activation frequencies to obtain a tetanic contraction [12]. Finally, for a given stimulation level, the pool of active MUs is fixed and depends on electrode location [13]. In the last two decades, several types of stimulation methods have been proposed to alter the MU recruitment specificities of electrically-induced contractions, with the ultimate goal to minimize fatigue. Two main approaches can be discerned. The first one aims at obtaining a physiological (i.e. Henneman-like) MU recruitment order by stimulating the muscle through spinal pathways [14]–[20]. The second one uses multiple stimulation sites to sequentially distribute muscle activation among different MU pools, thus reducing the stimulation frequency of each site. This type of stimulation can be achieved by positioning the stimulation electrodes at different locations on the muscle surface (distributed stimulation [21]–[29]), or by interleaving nStim and mStim ([30]–[35]). The latter is referred to as interleaved stimulation (iStim).

The extent to which multiple-site stimulation is effective in

reducing muscle fatigue depends on the degree of overlapping between the MU pools recruited at the different stimulation sites [32]. Ideally, if no overlap occurs between N stimulation sites, all MUs will be activated at 1/N of the overall stimulation frequency. The lower the proportion of MUs commonly activated by different sites (low overlap), the lower the average stimulation frequency of all activated MUs, which limits the occurrence of fatigue. The degree of overlap between MUs activated at different stimulation sites is overtly related to the electrode arrangement and to the anatomical features of the muscle: size, presence of different compartments, innervation paths. In large superficial muscles or muscle groups (e.g. quadriceps), multiple pairs of mStim electrodes positioned over different muscle regions (distributed stimulation) may be sufficient to selectively activate different muscle portions. However, a stimulation set-up based on several mStim sites may not be feasible in small muscles or may not be optimal in cases where a substantial fraction of the net joint force is generated by deep muscles or deep compartments of the same muscle. In these cases, iStim may be preferable, as the pool of MUs alternatively recruited by nStim and mStim are likely to differ in terms of MU type and spatial location. Okuma and colleagues [31] tested this hypothesis on the tibialis anterior muscle (TA), which is composed of a superficial and deep compartment separated by a central fascia (i.e. bipennate muscle [36]). By comparing the M-wave amplitude detected by fine-wire electrodes located in the superficial and deep compartments of TA, they showed that mStim preferentially activated the superficial muscle compartment, while nStim was not spatially selective. This stimulation-specific MU recruitment was considered to be the main determinant of the lower fatigue observed during TA stimulation with iStim [33]. Although fine-wire electromyography (EMG) is the only way to assess the electrical activation of deep muscle regions, this technique is limited by the small detection volume and does not provide a global description of muscle activation, which may be useful to better understand the extent to which superficial and deep muscle regions are selectively activated by different stimulation modalities.

An alternative approach to non-invasively quantify the contribution of both superficial and deep muscle compartments is ultrasonography (US), which may provide a direct measure of the tissue strain resulting from muscle activation [37], [38]. B-mode US gives the possibility to image skeletal muscle in static and dynamic conditions and characterize changes in muscle morphometric parameters such as fascicle length (FL), pennation angle (PA) and muscle thickness (MT) [39], [40]. In this study we used US image sequences to quantify architectural changes in the superficial and deep muscle compartments of TA during nStim and mStim at different contraction levels. We hypothesized that fascicular shortening and rotation would be prominent in the superficial compartment of the TA when using mStim, while nStim would elicit contraction patterns closer to voluntary contractions, similar in superficial and deep muscle compartments.

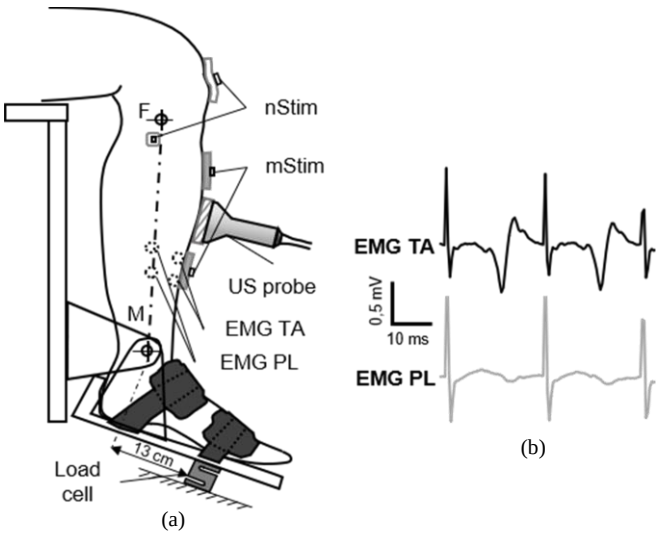

Fig. 1. (a) Schematic representation of the experimental setup. The lower leg was positioned in an isometric brace with a 90 deg knee angle and a 105 deg ankle angle. nStim and mStim indicate the electrode location for nerve stimulation and muscle stimulation, respectively (the cathode is the small electrode for nStim and the proximal electrode for mStim). Dotted circles represent the location of surface EMG electrodes positioned over tibialis anterior (TA) and peroneus longus (PL) to verify the selectivity of TA stimulation. F: head of fibula, M: malleolus. (b) Examples of M-waves detected from TA and PL during stimulation of the common peroneal nerve. The stimulation artifacts appear every 25 ms (40 pps stimulation). In this representative case, the difference in M-wave amplitude between TA and PA suggested a selective stimulation of TA.

II. Materials and Methods

A. Participants

Thirteen participants (age range: 24–45 years; mean height ± SD: 176 ± 8 cm; mean weight ± SD: 68 ± 7 kg), three females and ten males were recruited in the study. All subjects had no history of neurological or musculoskeletal impairments or diseases. The study was conducted in accordance with the Declaration of Helsinki and informed consent was obtained from all participants after receiving detailed explanation of the study procedures. Ethics approval (protocol n. 176866) was granted by the Ethics Committee of the University of Turin (Italy).

B. Protocol

1) Experimental procedure

Participants were seated on a chair with the backrest in front of an isometric pedal-like dynamometer. The position of the subject was adjusted to obtain approximately 110 deg of hip angle, 90 deg of knee angle and 105 deg of ankle angle (Fig. 1). The foot was securely blocked to the footplate of the dynamometer (see “Force recording”) with two blocking bindings.

At the beginning of the experiment, each participant performed three maximum voluntary contractions (MVCs) of the ankle dorsiflexors, while visual feedback of the force level and verbal encouragement were consistently provided. The maximum force level of the three MVCs was used to normalize force in the subsequent contractions [41].

Longitudinal US images were recorded from the TA during three types of isometric ankle dorsiflexions at 15% and 25% MVC force: voluntary (Vol), induced by mStim, and induced by nStim. The force levels used in this study were selected to be comparable to those often used in functional electrical stimulation protocols for foot drop [42]. Moreover, pilot experiments indicated that 25% of MVC force was the maximal level at which all data could reliably be collected, and all modalities of stimulations could be completed with negligible discomfort. For each subject and stimulation modality, the appropriate current amplitude inducing the required force level (15% and 25% MVC force) was identified before the beginning of the acquisitions.

For each contraction type and force level, three trials were acquired. During voluntary contractions the subject was provided with a visual force feedback and was asked to match a force profile on a screen: a 2-s ramp from zero to the target force (either 15% or 25% MVC force) followed by a 5-s constant level at the target force. The same force profile was used during electrically-evoked contractions, in this case the experimenter manually adjusted the stimulation current to match the required force.

2) Force recording

An isometric pedal-like dynamometer (OT Bioelettronica, Torino, Italy) housing a footplate connected with a force transducer (MODEL TF 031, full scale of 100 kg and sensitivity of 2 mv/V, CCT Transducers, Torino, Italy) was used to measure isometric forces. The output of the load cell was amplified with a general-purpose amplifier (Forza, OT Bioelettronica, Torino, Italy). A standard acquisition board (NI USB-6210, National Instruments, Austin, Texas) was used to acquire the analog output of the force amplifier, that was displayed in real time for feedback purposes on a computer screen, along with the required force profile. A custom-written MATLAB Graphical User Interface (The Mathwork, Natick, MA, USA) was used for this purpose.

3) Electrical stimulation

A constant-current neuromuscular stimulator (model DS7AH; Digitimer, Welwyn Garden City, UK) delivering a monophasic rectangular pulse with a duration of 100 μs was used for both mStim and nStim. The stimulation frequency was set to 40 pps through a stimulation trigger generator (StimTrig; LISiN, Politecnico di Torino, Italy) connected to the trigger input of the stimulator. Fig. 1a shows the positioning of stimulation electrodes. Disposable adhesive snap electrodes (EB Neuro S.p.A., Firenze, Italia) were used for both nStim and mStim.

For nStim, we positioned a small cathode electrode (1 × 1 cm) approximately 1 cm distally with respect to the head of the fibula along the peroneal nerve path and a large anode (7 × 4.5 cm) over the lateral aspect of the patella. It is worthy to note that the stimulation of the peroneal nerve may lead to the activation of both TA and peroneus longus (PL). Since we were interested in the association between architectural TA changes and dorsiflexion force, the activation of PL (generating foot eversion), had to be avoided. Therefore, we carefully adjusted the electrode configuration in order to maximize the stimulation of TA while minimizing that of PL. To this end, we detected bipolar M waves (DuePro, OT Bioelettronica, Torino, Italy) from TA and PL and we modified the pressure on the cathode (using an elastic strap) and its orientation to maximize the ratio between TA and PL M-wave amplitudes (Fig. 1b). In addition, for this type of stimulation, we also visually inspected the ankle movements: no or minimal ankle eversion should be visible during selective TA stimulation.

For mStim, the most proximal motor point over the TA muscle belly was identified following the procedure described in Botter et al. [42]. Afterwards, the cathode electrode (3.5 × 4.5 cm) was positioned over the identified motor point, while the anode electrode with the same size of the cathode was attached approximately 7 cm distally with respect to the cathode, to allow positioning of the US probe between them (Fig. 1a).

4) Ultrasound imaging

A MyLab X Vision ultrasound device (Esaote, Genova, Italy) equipped with a linear array transducer (LA532, 5 cm) with a frequency range of 3–13 MHz (set to 7.5 MHz to investigate skeletal muscle) was used to scan the TA. At the beginning of each experimental section, gain, depth, focus number, position and orientation were defined initially to achieve good quality of images on an individual basis. When the appropriate system set-up setting was found, all parameters were kept constant except for scanning depth and gain that were adjusted as needed. The ultrasound probe was hand-held between the stimulation electrodes for mStim and aligned with the proximal distal axis of the shank (Fig. 1a). The optimal position and orientation of the probe was set for each subject to clearly visualize the middle and deep aponeuroses, as well as single fascicles in the two muscle compartments (Fig. 2a) [43]. In this respect, special care was taken to identify the optimal medio-lateral tilting of the probe to an orientation perpendicular to the deeper aponeuroses of both compartments, to ensure measurement standardization and optimal imaging of fascicles (Fig 2b) [44]. When this adjustment could not be strictly obtained, the probe was set to match the wanted position as closely as possible to optimize the quality criteria described above.

For each contraction, an US video (sampling rate ~20 frames/s) was recorded and then transferred to a workstation for offline processing and later analysis.

C. Data analyses

Three morphometric parameters were extracted from the longitudinal US images, as described in the planimetric muscle model of the TA in Fig. 2a: FL, PA, MT. For each experimental condition and muscle compartment (superficial and deep) we computed changes in each variable with respect to the image of the rest phase, acquired in the same recording, starting 3 s before the contraction.

FL and PA were tracked semi-automatically with UltraTrack (version 4.2, [45]). The algorithm and the software have been described and validated previously [45]–[47]. The specific procedure adopted to identify the variables of interest (FL and

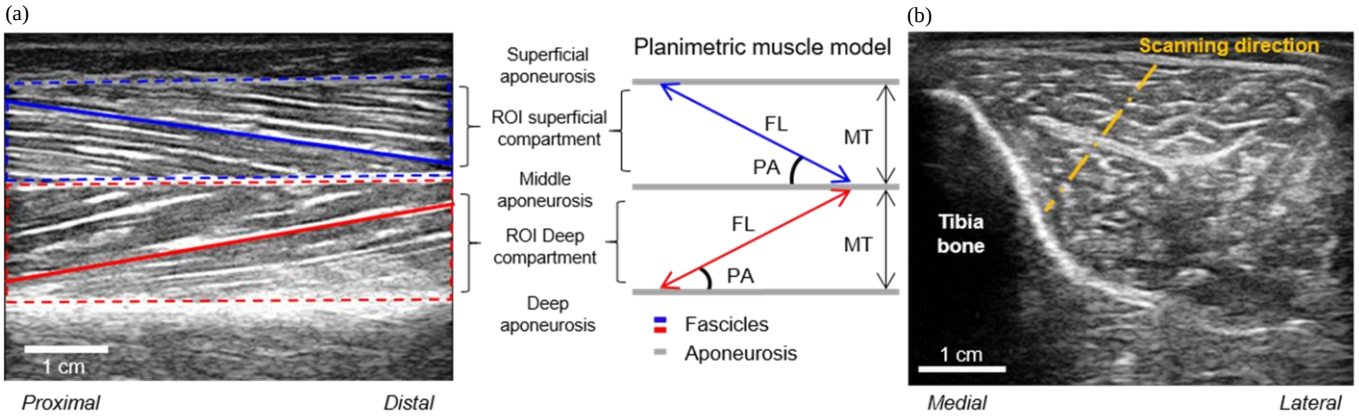

Fig. 2. (a) US longitudinal scan of TA. All the aponeuroses are clearly visible and consequently the two compartments (superficial in blue and deep in red). For each muscle compartment one fascicle (solid line) and the region of interest (dashed lines) are highlighted. Planimetric muscle model of the longitudinal US image reporting all the morphometric variables considered. FL = fascicle length; PA = pennation angle; MT = muscle thickness. (b) Trasversal US image of TA to visually inspect the scanning direction (yellow dash-dotted line) and achieve good quality of the longitudinal image. It is possible to notice the deep and central aponeurosis and the tibia bone.

PA) is described in Farris and Lichtwark [45]. MT was calculated from the central parts of the regions of interests defined between the aponeuroses of each muscle compartments (Fig. 2a). When the length of fascicles extended beyond the field of view, the missing fascicle portion was estimated using linear extrapolations of the fascicle and aponeuroses. The PA was calculated as the sum of the angle of fascicles relative to the image horizontal axis and the angle between this axis and the central or deep aponeuroses [48].

1) Statistical analysis

The Shapiro-Wilk normality test was used to verify the normal distribution of the data. As the normal distribution was confirmed for all datasets, non-parametric statistical tests were adopted and results are reported as means ± SD. In order to verify the validity of the subsequent comparisons (similar mechanical output), a one-way ANOVA was used to compare force variables (rising time and force level) between the different contraction types. The effects of the factors (i) contraction type (Vol, nStim, mStim), (ii) TA compartment (superficial and deep) and (iii) contraction level (15% and 25% MVC) on architectural variables (MT, FL, PA) were assessed using a three-way repeated measures ANOVA. Bonferroni correction was performed whenever the ANOVA indicated a significant, additive effect. A level of $p < 0.05$ was selected to indicate statistical significance.

III. Results

A. General Description

All tested subjects completed the experiment without reporting excessive discomfort due to electrical stimulation. In eleven subjects, the peak-to-peak amplitude of the M wave induced in TA was at least 10 times larger than that of the PL, suggesting a good stimulation selectivity for TA. In two participants, the ratio between the amplitude of EMG signals detected from TA and PL during nStim was approximately 3. For this reason, these two subjects were excluded from further analyses. For the remaining eleven subjects, the selective stimulation of TA was also confirmed by visual inspection of the foot movement during the test contractions, showing no foot eversion in all of them. In one subject, the electrode configuration was slightly changed to achieve a selective contraction of the TA during peroneal nerve trunk stimulation. Specifically, we kept the cathode electrode in the original position over the nerve and we moved the large electrode (i.e., the anode) from the patella to the posterior distal thigh to modify the direction of the current lines under the cathode electrode, which likely determined a more selective activation of the TA.

Table 1 reports the current levels corresponding to the motor thresholds and those required to reach the plateau of the target forces, for the two stimulation modalities. As expected, both for nStim and mStim, significantly higher current intensities were required to reach 25% MVC than 15% MVC ($p<0.05$ Wilcoxon signed-rank test). For both contraction levels, current amplitudes in mStim were higher than nStim ($p<0.05$ Wilcoxon signed-rank test).

TABLE I
CURRENT AMPLITUDES (MEAN ± SD) IN 11 SUBJECTS

	Mot Thr*	15% MVC	25% MVC
mStim (mA)	29.7 ± 7.0	52.1 ± 8.3	66.5 ± 8.1
nStim (mA)	14.9 ± 5.1	20.0 ± 6.6	21.4 ± 7.6

*Mot Thr = motor threshold

The average MVC force of all the subjects was 257±35 N and considering the lever arm of the load cell axis from the rotation axis of 0.13 m (Fig. 1a), the mean torque was 33.4±4.6 Nm. For both contraction levels (15% and 25% MVC), the force profiles of the three types of contraction were comparable (Fig. 3). The rising time, defined as the time interval between the 10% and 90% of the required force, was 2.1±0.5 s for Vol, 2.9±1.5 s for mStim and 2.4±1.6 s for nStim at 15% MVC and 2.0±0.3 s for Vol, 2.7±1.0 s for mStim and 2.0±1.0 s for nStim at 25% MVC. The average force level (% MVC) in the constant-force phase (Fig. 3) was 15.0±0.4% for Vol, 15.2±1.3% for mStim and 15.5±0.9% for nStim at 15% MVC and 24.7±0.6% for Vol, 25.7±3.2% for mStim and

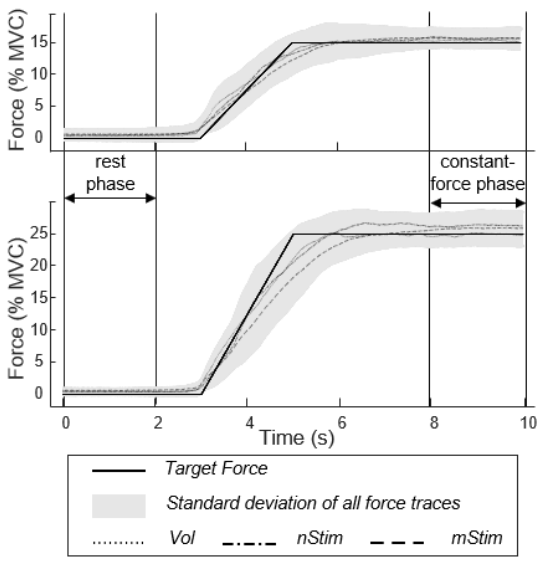

Fig. 3. Average force profiles for each contraction type at 15% MVC (upper panel) and 25% MVC (lower panel). The target profiles (black solid lines) were displayed in real time. The grey areas are the standard deviation of all force traces. Vol, nStim and mStim are the average force profiles across subjects for the three contraction types.

26.4±1.8% for nStim at 25% MVC. All rising times and relative forces were similar between the three contraction types (p>0.05) for the same contraction level.

B. Architectural changes induced by Vol, nStim and mStim contractions

Figure 4 shows the architectural changes induced by the three types of contraction on a representative subject. The absolute values of the architectural variables during 25% MVC contractions are displayed using a planimetric model of the TA muscle. The figure shows that during mStim, TA fascicles underwent a greater shortening compared to that observed during nStim and Vol. During mStim, changes in PA of the superficial compartment were more pronounced that those observed for Vol and nStim, while similar values were observed across contraction types for the deep compartment. Similar values of PA and FL were observed for Vol and nStim conditions.

The representative results reported in Figure 4 were confirmed by the analysis of pooled data from all subjects (Table 2). Figure 5 shows the effects of contraction type on percentage changes of architectural variables: MT (a), FL (b), PA (c) for superficial and deep TA and for both contraction levels (15% and 25% MVC) in 11 subjects. As expected, for all contraction types and for both compartments, FL decreased and PA increased, indicating respectively fascicle shortening and increase of pennation angle. Overall, absolute changes of PA and FL seemed more pronounced for the superficial compartment than for the deep one, resulting in larger MT changes of the superficial TA.

The three-way ANOVA indicated a significant effect of the compartment (i.e. superficial and deep) on all variables ($p<0.001$) and an effect of the force level and contraction type on FL and PA ($p<0.01$) but not on MT ($p>0.05$). The interaction between contraction type and force level was significant for FL ($p<0.01$) but not for PA ($p=0.06$). Significant interactions between contraction type and compartment were found for FL ($p<0.01$) and PA ($p<0.001$). No interaction effects were found for MT ($p>0.05$, Fig. 5a).

For both force levels, significant differences were found in the superficial compartment between mStim and the other two contraction types on FL ($p<0.001$) and PA ($p<0.001$). Specifically, fascicles shortened more with mStim (-14.1% at 15% MVC, -19.9% at 25% MVC) than with Vol (-9.2% at 15% MVC, -10.9% at 25% MVC) and nStim (-8.1% at 15% MVC, -10.3% at 25% MVC) contractions (Fig. 5b).

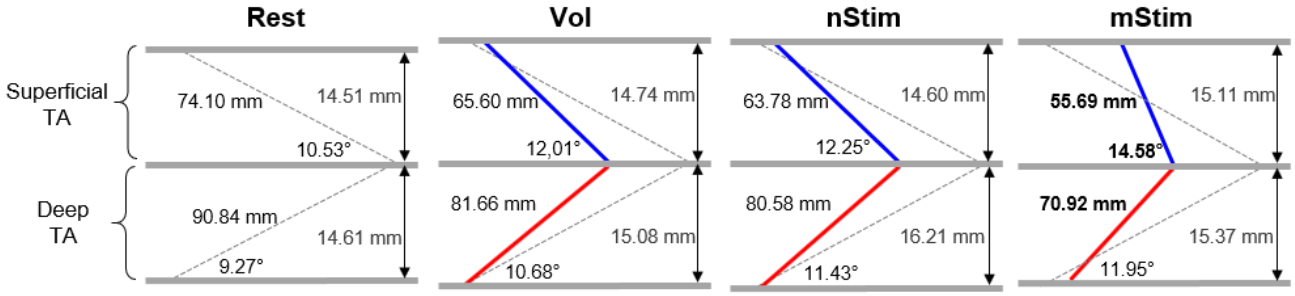

Fig. 4. Architectural changes induced by Vol, nStim and mStim contractions of TA at 25% MVC in one representative subject. Pennation Angle (PA), Fascicle Length (FL) and Muscle Thickness (MT) are represented on a planimetric model of the superficial and deep TA compartments. Blue and red lines represent muscle fascicles. The inclination of the representing muscle fascicles was emphasized for representation purposes.

TABLE II
ABSOLUTE CHANGES OF ARCHITECTURAL VARIABLES WITH RESPECT TO THE REST CONDITION (MEAN ± SD)

Contr type	%MVC	MT sup (mm)	MT deep (mm)	FL sup (mm)	FL deep (mm)	PA sup (°)	PA deep (°)
Vol	15%	0.8 ± 0.6	0.0 ± 0.5	-6.3 ± 2.6	-5.5 ± 2.1	1.7 ± 0.6	0.8 ± 0.6
nStim	15%	1.2 ± 0.8	0.1 ± 0.9	-5.8 ± 2.2	-5.9 ± 2.9	1.7 ± 0.7	1.3 ± 0.9
mStim	15%	1.1 ± 0.9	0.0 ± 1.0	-11.0 ± 4.3	-8.1 ± 4.4	3.0 ± 0.9	1.2 ± 0.9
Vol	25%	1.0 ± 0.8	0.5 ± 0.8	-8.0 ± 3.1	-6.9 ± 2.8	2.3 ± 0.6	1.2 ± 0.7
nStim	25%	1.2 ± 1.1	0.6 ± 1.2	-8.2 ± 3.7	-6.4 ± 2.8	2.1 ± 1.1	1.4 ± 0.9
mStim	25%	1.5 ± 1.0	0.2 ± 0.8	-14.5 ± 3.6	-11.2 ± 5.0	4.4 ± 0.5	1.8 ± 0.9
Average at rest		15.5 ± 2.2	18.6 ± 2.6	69.3 ± 16.2	78.0 ± 13.9	12.2 ± 2.2	12.8 ± 2.6

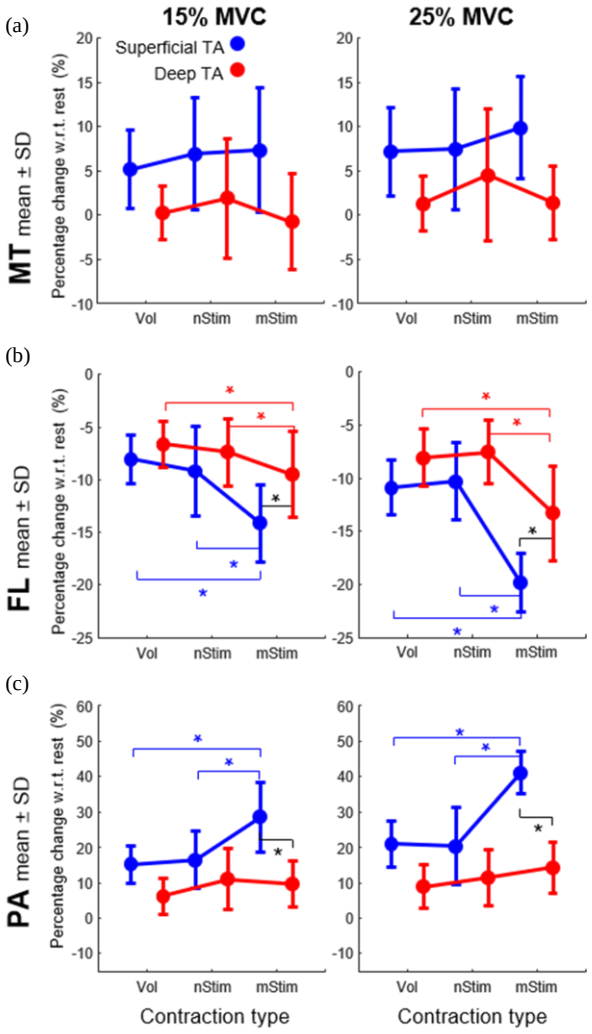

Fig. 5. Percentage changes with respect to rest (mean ± standard deviation of 11 subjects) of a) muscle thickness (MT), b) fascicle length (FL), c) pennation angle (PA), for each contraction type of superficial (blue) and deep (red) compartments of TA. * denotes statistically significant differences ($p<0.05$).

Consistently, the increase in PA was greater with mStim (28.5% at 15% MVC, 41.1% at 25% MVC) than with Vol (15.2% at 15% MVC, 21.0% at 25% MVC) and nStim (16.5% at 15% MVC, 20.3% at 25% MVC) contractions (Fig. 5c).

In the deep compartment, significant differences appeared only for FL ($p<0.001$). As observed for the superficial compartment, fascicle shortening was greater with mStim (-9.5% at 15% MVC, -13.3% at 25% MVC) than with Vol (-6.7% at 15% MVC, -8.0% at 25% MVC) and nStim (-7.4% at 15% MVC, -7.6% at 25% MVC) contractions (Fig. 5b). Instead, changes in PA were comparable between contractions types in the deep compartment (15% MVC: 6.2% Vol, 11.1% nStim, 9.8% mStim; 25% MVC: 8.1% Vol, 11.5% nStim, 14.3% mStim). For mStim contractions, both FL and PA showed significant differences between the superficial and deep compartment ($p<0.01$).

IV. Discussion

A major concern in several rehabilitation protocols and interventions including electrical stimulation is to induce a physiological muscle response. In the present study we compared the architectural changes of the superficial and deep TA occurring during voluntary contractions versus electrical stimulation applied to the nerve trunk (nStim) and to the terminal axonal branches at the muscle level (mStim). Our findings indicate that architectural changes elicited with nerve stimulation in the deep and superficial compartments were similar to those observed during voluntary contractions at the same contraction level. By contrast, nearly all architectural changes induced by muscle belly electrical stimulation differed from the contractile behaviour of voluntary contractions, both in absolute magnitude and in their relative differences between compartments. These observations suggest that the distinct pattern of spatial MU recruitment elicited with nStim better matches voluntary contractile behaviour than with mStim.

The possibility to selectively activate different MU populations during electrical stimulation is intriguing as it potentially allows to implement stimulation paradigms aimed at promoting a more physiological response which may in turn reduce the development of muscle fatigue. Indeed, a temporal sharing of the force production among different groups of MUs would allow to stimulate each group at a lower frequency thus limiting the occurrence of fatigue [33]. With interleaved stimulation [32], [33], [35], the selective activation of different populations of MUs is based on the hypothesis that, by stimulating the nerve (nStim), MU recruitment is distributed evenly throughout the muscle volume, while muscle belly stimulation (mStim) preferentially activates superficial MUs. In this study we tested this hypothesis by analysing how the superficial and deep fascicles of the TA respond to mStim and nStim. We chose the TA muscle because of its relevance for FES applications [2], [3], [42], [49], [50]. Moreover, its bipennate structure is particularly convenient to study the mechanical activation of superficial and deep muscle regions [43], [49]. Our results revealed that: (i) Vol and nStim contractions induced comparable architectural changes in superficial and deep TA for both contraction levels; (ii) as compared to Vol and nStim, mStim contractions induced greater FL changes in both compartments and greater PA changes only in the superficial compartment; (iii) architectural changes induced by mStim in the superficial TA compartment were significantly greater than in the deep compartment with respect to Vol and nStim. Basically, Fig. 4 and 5 show that nStim led to a similar behaviour in terms of architectural changes than Vol, whereas mStim did not. All the architectural changes were more pronounced for the higher contraction level (25% MVC) which can be explained by the greater MU recruitment required to reach the target force. By providing a quantitative description of muscle mechanics during different type of electrically-induced contractions, our study complement and integrate the electrophysiological observations of the group of Collins [31], which support the

combined use of muscle and nerve stimulation (interleaved stimulation) as a valid physiological alternative to stimulate different populations of TA MUs.

A quantitative comparison between our results and those observed by other studies in the literature is not straightforward because of differences in the experimental conditions and extracted variables. To the best of our knowledge, previous studies had thus far only been performed during voluntary contractions. Maganaris and Baltzopoulos [43] and Raiteri et al. [51], [52] have described the fascicular contractile behaviour for both compartments of the TA, while a few other studies focused on the superficial compartment only [37], [41], [53]. Despite the different experimental configurations, isometric contractions were characterised by an increase in PA and a decrease in FL in all the above-mentioned papers, as observed in our study. Raiteri et al. evaluated FL and PA at various isometric force levels [51] and ankle positions [52] during voluntary contractions. Similarly to our observations, they found a significant effect of the contraction level in both FL and PA, although compartment-specific changes were found only for PA and not for FL. The increase in muscle thickness shown from our results (~5% in the superficial compartment only) is also in line with most previous studies [37], [41], [52], yet not all [43], which have measured an increase of the thickness of the entire muscle comparable to the variations obtained in our study. The lack of thickening of the deep compartment for all contraction types was an unexpected result. It is worth noting however, that although US images suggest that TA can be treated as a symmetrically bipennate muscle [43], [51], changes in MT of the deep compartment may be limited by anatomical constraints. For instance, the presence of the tibia bone may limit the thickening of the deep TA in the plane of the US images. Another factor possibly accounting for the small and highly variable MT changes is that MT is the result of the combination of both FL and PA [54], that may or may not result in muscle thickening, especially for low contraction levels.

As shown in Fig. 5b and 5c, mStim was the contraction type inducing greater FL and PA changes (see also absolute values in Table 2). We attribute this observation to the fact that the active muscle tissue is restricted to a smaller volume with mStim than with voluntary and nStim contractions. With mStim, the activated region is restricted to the superficial muscle compartment and to the muscle region limited proximally by the cathode. It is therefore reasonable to expect that this region of the muscle undergoes a greater shortening with mStim to compensate for the missing contribution of the inactive regions. In contrast, nStim induces a contractile behaviour closer to voluntary contractions, by virtue of an even recruitment of the muscle along the proximo-distal axis. The regional bias of activation attributed to mStim also seems to occur in the antero-posterior direction, with between-compartment differences in contractile behaviour at both contraction levels. Relative differences in fascicular shortening and rotation between fascicles were not observed with other modalities or contraction intensities (Fig. 5b). Previous work also supports the physiological trend for both compartments of the TA muscle to present symmetrical changes in architecture under isometric contractions at various intensities [52]. The contractile asymmetry between compartments seen with mStim indicates that the superficial muscle region is relatively more activated than the deep one. For this reason, the changes in architecture occurring in the deep compartment may partly result from the strain of the superficial compartment.

The position of the electrodes with respect to the anatomical structures (i.e. nerve/nerve branches) plays an essential role in determining the muscle response to both nStim and mStim [1], [3], [6], [7], [13]. It is therefore reasonable to question whether and to what extent the results of this study depend on the electrode configuration used for nStim and, most importantly, for mStim. For instance, a recent study showed that the knee extension torque was positively associated with the distance between stimulation electrodes over the quadriceps muscle belly [55]. The Authors of this study suggested that with a larger inter-electrode distance, current pathways may reach a larger fraction of terminal nerve branches possibly including those innervating deep muscle regions, despite using surface electrodes. If the observed regional bias of activation of mStim were due to the selected inter-electrode distance, the involvement of deep muscle regions could potentially be obtained by increasing this parameter without resorting to nerve stimulation. Although this option was not tested in this study, the anatomy and the innervation pathways of TA make this hypothesis unlikely. Yu et al. [56] showed that the superficial and deep TA compartments are innervated by two to four branches of the deep peroneal nerve. In this muscle, the antero-superior (i.e. superficial) compartment is innervated by one or two anterior nerve branches, while the posterior branches innervate the postero-inferior (i.e. deep) compartment. The two pairs of branches innervating superficial and deep TA split proximally before entering in the muscle in the postero-lateral side [49], and there is no evidence of motor axons crossing the central aponeurosis separating the two muscle compartments. Therefore, the electrical excitation of deep intramuscular nerve branches appears difficult to achieve from the surface electrodes positioned over the muscle belly (i.e. mStim), In this regard, imaging techniques, such as PET [57], [58], could be useful to determine if and to what extent the deep TA compartment can be activated by mStim. It is important to underline that all the above considerations are specific to the TA, the generalization of the outcomes of this study to other muscle groups cannot be done a priori or requires a careful evaluation of their specific anatomy.

A final, methodological remark concerns the stimulation of muscles other than TA during our experimental protocol. The fact that the common peroneal nerve divides into a deep branch (that innervates TA, extensor hallucis longus and extensor digitorum longus), and a superficial branch (that innervates PL, and fibularis brevis) is noteworthy. Considering

that our stimulation method was aimed at eliciting dorsiflexion, we can exclude a substantial involvement of the nerve branch innervating PL and fibularis brevis, but other muscles innervated by the deep branch could have contributed to the measured force. However, the contribution of extensor hallucis and digitorum longus would remain negligible compared to that of TA, because the foot was blocked on the footplate by bindings locking the tarsometatarsal joints.

V. Conclusion

In the present study we showed that in tibialis anterior nerve stimulation results in a distributed MU recruitment over the entire muscle volume, similarly to voluntary contractions, whereas mStim preferentially activates the superficial muscle layer. Although our results do not allow to infer on the recruitment in terms of motor unit type, two practical implications arise from our results. Voluntary and nStim contractions activate motor units that are similarly distributed throughout the muscle, which makes the two contractions comparable from a biomechanical point of view, a feature that could be desirable during electrical stimulation. On the other hand, the observed diversity between spatial recruitment of nStim and mStim implies the involvement of different motor unit populations, which in turn justifies strategies based on interleaved nerve/muscle stimulation to reduce muscle fatigue during electrically-induced contractions.

Acknowledgment

The authors are grateful to Prof. Silvestro Roatta (University of Turin, Turin, Italy) for providing the ultrasound device.

References

[1] N. A. Maffiuletti, “Physiological and methodological considerations for the use of neuromuscular electrical stimulation,” *Eur. J. Appl. Physiol.*, vol. 110, no. 2, pp. 223–234, 2010.

[2] G. M. Lyons, T. Sinkjær, J. H. Burridge, and D. J. Wilcox, “A review of portable FES-based neural orthoses for the correction of drop foot,” *IEEE Trans. Neural Syst. Rehabil. Eng.*, vol. 10, no. 4, pp. 260–279, 2002.

[3] B. . B. M. Doucet, A. Lam, and L. Griffin, “Neuromuscular Electrical Stimulation for Skeletal Muscle Function,” *Yale J. Biol. Med.*, vol. 85, no. 2, pp. 201–215, 2012.

[4] B. M. Kluger, L. B. Krupp, and R. M. Enoka, “Fatigue and fatigability in neurologic inllnesses,” *Neurology*, vol. 80, pp. 409–416, 2013.

[5] E. Henneman, “Relation between size of neurons and their susceptibility to discharge,” *Science (80-.).*, vol. 126, no. 3287, pp. 1345–1347, 1957.

[6] R. M. Enoka, “Activation order of motor axons in electrically evoked contractions,” *Muscle and Nerve*, vol. 25, no. 6, pp. 763–764, 2002.

[7] M. Knaflitz, R. Merletti, and C. J. De Luca, “Inference of motor unit recruitment order in voluntary and electrically elicited contractions,” *J. Appl. Physiol.*, vol. 68, no. 4, pp. 1657–1667, 1990.

[8] M. Jubeau, J. Gondin, A. Martin, A. Sartorio, and N. A. Maffiuletti, “Random motor unit activation by electrostimulation,” *Int. J. Sports Med.*, vol. 28, no. 11, pp. 901–4, 2007.

[9] A. Botter, R. Merletti, and M. A. Minetto, “Pulse charge and not waveform affects M-wave properties during progressive motor unit activation,” *J. Electromyogr. Kinesiol.*, vol. 19, no. 4, pp. 564–573, 2009.

[10] P. Feiereisen, J. Duchateau, and K. Hainaut, “Motor unit recruitment order during voluntary and electrically induced contractions in the tibialis anterior,” *Exp. Brain Res.*, vol. 114, no. 1, pp. 117–123, 1997.

[11] G. R. Adams, R. T. Harris, D. Woodard, and G. A. Dudley, “Mapping of electrical muscle stimulation using MRI,” *J. Appl. Physiol.*, vol. 74, no. 2, pp. 532–537, 1993.

[12] C. S. Bickel, C. M. Gregory, and J. C. Dean, “Motor unit recruitment during neuromuscular electrical stimulation: A critical appraisal,” *Eur. J. Appl. Physiol.*, vol. 111, pp. 2399–2407, 2011.

[13] M. Vanderthommen, J. C. Depresseux, L. Dauchat, C. Degueldre, J. L. Croisier, and J. M. Crielaard, “Spatial distribution of blood flow in electrically stimulated human muscle: A positron emission tomography study,” *Muscle and Nerve*, vol. 23, no. 4, pp. 482–489, 2000.

[14] J. L. Dideriksen, S. Muceli, S. Dosen, C. M. Laine, and D. Farina, “Physiological recruitment of motor units by high-frequency electrical stimulation of afferent pathways,” *J. Appl. Physiol.*, vol. 118, no. 3, pp. 365–376, 2015.

[15] A. J. Bergquist, M. J. Wiest, Y. Okuma, and D. F. Collins, “H-reflexes reduce fatigue of evoked contractions after spinal cord injury,” *Muscle and Nerve*, vol. 50, no. 2, pp. 224–234, 2014.

[16] J. Dideriksen, K. Leerskov, M. Czyzewska, and R. Rasmussen, “Relation between the frequency of short-pulse electrical stimulation of afferent nerve fibers and evoked muscle force,” *IEEE Trans. Biomed. Eng.*, vol. 64, no. 11, pp. 2737–2745, 2017.

[17] N. A. Maffiuletti, M. Pensini, G. Scaglioni, A. Ferri, Y. Ballay, and A. Martin, “Effect of electromyostimulation training on soleus and gastrocnemii H- and T-reflex properties,” *Eur. J. Appl. Physiol.*, vol. 90, no. 5–6, pp. 601–607, 2003.

[18] A. J. Bergquist *et al.*, “Neuromuscular electrical stimulation: implications of the electrically evoked sensory volley,” *Eur. J. Appl. Physiol.*, vol. 111, no. 10, p. 2409, 2011.

[19] J. C. Dean, J. M. Clair-Auger, O. Lagerquist, and D. F. Collins, “Asynchronous recruitment of low-threshold motor units during repetitive, low-current stimulation of the human tibial nerve,” *Front. Hum. Neurosci.*, vol. 8, no. 1002, pp. 1–12, 2014.

[20] J. Duclay and A. Martin, “Evoked H-reflex and V-wave responses during maximal isometric, concentric, and eccentric muscle contraction,” *J. Neurophysiol.*, vol. 94, no. 5, pp. 3555–3562, 2005.

[21] D. G. Sayenko, M. R. Popovic, and K. Masani, “Spatially distributed sequential stimulation reduces muscle fatigue during neuromuscular electrical stimulation,” *Proc. Annu. Int. Conf. IEEE Eng. Med. Biol. Soc. EMBS*, no. 4, pp. 3614–3617, 2013.

[22] R. Ruslee, J. Miller, and H. Gollee, “Investigation of different stimulation patterns with doublet pulses to reduce muscle fatigue,” *J. Rehabil. Assist. Technol. Eng.*, vol. 6, 2019.

[23] N. M. Malešević, L. Z. Popović, L. Schwirtlich, and D. B. Popović, “Distributed low-frequency functional electrical stimulation delays muscle fatigue compared to conventional stimulation,” *Muscle and Nerve*, vol. 42, no. 4, pp. 556–562, 2010.

[24] L. Z. Popović and N. M. Malešević, “Muscle fatigue of quadriceps in paraplegics: Comparison between single vs. multi-pad electrode surface stimulation,” *Proc. 31st Annu. Int. Conf. IEEE Eng. Med. Biol. Soc. Eng. Futur. Biomed. EMBC 2009*, pp. 6785–6788, 2009.

[25] M. Laubacher, A. E. Aksöz, R. Riener, S. Binder-Macleod, and K. J. Hunt, “Power output and fatigue properties using spatially distributed sequential stimulation in a dynamic knee extension task,” *Eur. J. Appl. Physiol.*, vol. 117, no. 9, pp. 1787–1798, 2017.

[26] A. J. Bergquist, V. Babbar, S. Ali, M. R. Popovic, and K. Masani, “Fatigue reduction during aggregated and distributed sequential stimulation,” *Muscle and Nerve*, vol. 56, no. 2, pp. 271–281, 2017.

[27] A. J. Buckmire, D. R. Lockwood, C. J. Doane, and A. J. Fuglevand, “Distributed stimulation increases force elicited with functional electrical stimulation,” *J. Neural Eng.*, vol. 15, no. 2, p. 026001, 2018.

[28] D. Morgan, Y. Huang, A. Wise, U. Proske, and I. E. Brown, “Distributed stimulation of skeletal muscle,” *Proc. Inaug. Conf. Vic. Chapter IEEE Eng. Med. Biol. Soc.*, pp. 112–115, 1999.

[29] L. Z. P. Maneski, N. M. Malešević, A. M. Savić, T. Keller, and D. B. Popović, “Surface-distributed low-frequency asynchronous stimulation delays fatigue of stimulated muscles,” *Muscle Nerve*, vol. 48, no. 6, pp. 930–937, 2013.

[30] M. J. Wiest, A. J. Bergquist, and D. F. Collins, “Torque, Current, and Discomfort During 3 Types of Neuromuscular Electrical Stimulation of Tibialis Anterior,” *Am. J. Ophthalmol.*, vol. 97, no. 8,

pp. 790–798, 2017.
[31] Y. Okuma, A. J. Bergquist, M. Hong, K. M. Chan, and D. F. Collins, “Electrical stimulation site influences the spatial distribution of motor units recruited in tibialis anterior,” *Clin. Neurophysiol.*, vol. 124, no. 11, pp. 2257–2263, 2013.
[32] M. J. Wiest, A. J. Bergquist, H. L. Schimidt, K. E. Jones, and D. F. Collins, “Interleaved neuromuscular electrical stimulation: Motor unit recruitment overlap,” *Muscle and Nerve*, vol. 55, no. 4, pp. 490–499, 2017.
[33] J. W. H. Lou, A. J. Bergquist, A. Aldayel, J. Czitron, and D. F. Collins, “Interleaved neuromuscular electrical stimulation reduces muscle fatigue,” *Muscle and Nerve*, vol. 55, no. 2, pp. 179–189, 2017.
[34] S. Regina Dias Da Silva, D. Neyroud, N. A. Maffiuletti, J. Gondin, and N. Place, “Twitch potentiation induced by two different modalities of neuromuscular electrical stimulation: Implications for motor unit recruitment,” *Muscle and Nerve*, vol. 51, no. 3, pp. 412–418, 2015.
[35] A. J. Bergquist, M. J. Wiest, Y. Okuma, and D. F. Collins, “Interleaved neuromuscular electrical stimulation after spinal cord injury,” *Muscle and Nerve*, vol. 56, no. 5, pp. 989–993, 2017.
[36] D. C. Bland, L. A. Prosser, L. A. Bellini, K. E. Alter, and D. L. Damiano, “Tibialis anterior architecture, strength and gait in individuals with cerebral palsy,” *Muscle Nerve*, vol. 44, no. 4, pp. 509–517, 2012.
[37] P. W. Hodges, L. H. M. Pengel, R. D. Herbert, and S. C. Gandevia, “Measurement of muscle contraction with ultrasound imaging,” *Muscle and Nerve*, vol. 27, no. 6, pp. 682–692, 2003.
[38] I. D. Loram, C. N. Maganaris, and M. Lakie, “Use of ultrasound to make noninvasive in vivo measurement of continuous changes in human muscle contractile length,” *J. Appl. Physiol.*, vol. 100, no. 4, pp. 1311–1323, 2006.
[39] G. Q. Zhou, P. Chan, and Y. P. Zheng, “Automatic measurement of pennation angle and fascicle length of gastrocnemius muscles using real-time ultrasound imaging,” *Ultrasonics*, vol. 57, pp. 72–83, 2015.
[40] C. N. Maganaris, V. Baltzopoulos, and A. J. Sargeant, “In vivo measurements of the triceps surae complex architecture in man: Implications for muscle function,” *J. Physiol.*, vol. 512, no. 2, pp. 603–614, 1998.
[41] M. Ruiz Muñoz, M. González-Sánchez, and A. I. Cuesta-Vargas, “Tibialis anterior analysis from functional and architectural perspective during isometric foot dorsiflexion: A cross-sectional study of repeated measures,” *J. Foot Ankle Res.*, vol. 8, no. 1, pp. 1–9, 2015.
[42] T. Watanabe, S. Endo, and R. Morita, “Development of a prototype of portable FES rehabilitation system for relearning of gait for hemiplegic subjects,” *Healthc. Technol. Lett.*, vol. 3, no. 4, pp. 284–289, 2016.
[43] C. N. Maganaris and V. Baltzopoulos, “Predictability of in vivo changes in pennation angle of human tibialis anterior muscle from rest to maximum isometric dorsiflexion,” *Eur. J. Appl. Physiol. Occup. Physiol.*, vol. 79, no. 3, pp. 294–297, 1999.
[44] M. R. Bénard, J. G. Becher, J. Harlaar, P. A. Huijing, and R. T. Jaspers, “Anatomical information is needed in ultrasound imaging of muscle to avoid potentially substantial errors in measurement of muscle geometry,” *Muscle and Nerve*, vol. 39, no. 5, pp. 652–65, 2009.
[45] D. J. Farris and G. A. Lichtwark, “UltraTrack: Software for semi-automated tracking of muscle fascicles in sequences of B-mode ultrasound images,” *Comput. Methods Programs Biomed.*, vol. 128, pp. 111–118, 2016.
[46] N. J. Cronin, C. P. Carty, R. S. Barrett, and G. Lichtwark, “Automatic tracking of medial gastrocnemius fascicle length during human locomotion,” *J. Appl. Physiol.*, vol. 111, no. 5, pp. 1491–1496, 2011.
[47] J. G. Gillett, R. S. Barrett, and G. A. Lichtwark, “Reliability and accuracy of an automated tracking algorithm to measure controlled passive and active muscle fascicle length changes from ultrasound,” *Comput. Methods Biomech. Biomed. Engin.*, vol. 16, no. 6, pp. 678–687, 2013.
[48] O. R. Seynnes and N. J. Cronin, “Simple Muscle Architecture Analysis (SMA): an ImageJ macro tool to automate measurements in B-mode ultrasound scans,” *PLoS One*, vol. 15, no. 2, 2020.
[49] K. H. Yi, L. Cong, J. H. Bae, E. S. Park, D. wook Rha, and H. J. Kim, “Neuromuscular structure of the tibialis anterior muscle for functional electrical stimulation,” *Surg. Radiol. Anat.*, vol. 39, no. 1, pp. 77–83, 2017.
[50] F. Bethoux *et al.*, “The effects of peroneal nerve functional electrical stimulation versus ankle-foot orthosis in patients with chronic stroke: A randomized controlled trial,” *Neurorehabil. Neural Repair*, vol. 28, no. 7, pp. 688–697, 2014.
[51] B. J. Raiteri, A. G. Cresswell, and G. A. Lichtwark, “Muscle-Tendon length and force affect human tibialis anterior central aponeurosis stiffness in vivo,” *Proc. Natl. Acad. Sci. U. S. A.*, vol. 115, no. 14, pp. E3097–E3105, 2018.
[52] B. J. Raiteri, A. G. Cresswell, and G. A. Lichtwark, “Three-dimensional geometrical changes of the human tibialis anterior muscle and its central aponeurosis measured with three-dimensional ultrasound during isometric contractions,” *PeerJ*, vol. 2016, no. 7, 2016.
[53] R. D. Herbert, A. M. Moseley, J. E. Butler, and S. C. Gandevia, “Change in length of relaxed muscle fascicles and tendons with knee and ankle movement in humans,” *J. Physiol.*, vol. 539, no. 2, pp. 637–645, 2002.
[54] J. M. Wakeling, O. M. Blake, I. Wong, M. Rana, and S. S. M. Lee, “Movement mechanics as a determinate of muscle structure, recruitment and coordination,” *Philos. Trans. R. Soc. B Biol. Sci.*, vol. 366, no. 1570, pp. 1554–1564, 2011.
[55] T. M. Vieira, P. Potenza, L. Gastaldi, and A. Botter, “Electrode position markedly affects knee torque in tetanic, stimulated contractions,” *Eur. J. Appl. Physiol.*, vol. 116, no. 2, pp. 335–342, 2016.
[56] D. Yu, H. Yin, T. Han, H. Jiang, and X. Cao, “Intramuscular innervations of lower leg skeletal muscles: applications in their clinical use in functional muscular transfer,” *Surg. Radiol. Anat.*, vol. 38, no. 6, pp. 675–685, 2016.
[57] B. Haddock *et al.*, “Assessment of muscle function using hybrid PET/MRI: comparison of 18F-FDG PET and T2-weighted MRI for quantifying muscle activation in human subjects,” *Eur. J. Nucl. Med. Mol. Imaging*, vol. 44, no. 4, pp. 704–711, 2017.
[58] T. Rudroff, K. K. Kalliokoski, D. E. Block, J. R. Gould, W. C. Klingensmith, and R. M. Enoka, “PET/CT imaging of age- and task-associated differences in muscle activity during fatiguing contractions,” *J. Appl. Physiol.*, vol. 114, no. 9, pp. 1211–1219, 2013.